Parrondo effect in quantum coin-toss simulations

Joel Weijia Lai
Science and Math Cluster, Singapore University of Technology and Design, 8 Somapah Road, Singapore S487372

Kang Hao Cheong*
Science and Math Cluster, Singapore University of Technology and Design, 8 Somapah Road, Singapore S487372 and SUTD-Massachusetts Institute of Technology International Design Centre, Singapore S487372

(Received 13 January 2020; accepted 28 April 2020; published 18 May 2020)

Game A + Game B = Game C. Parrondo's games follow this basic structure where A and B are losing games and C is a winning game—a phenomenon called Parrondo's paradox. These games can take on a wider class of definitions and exhibit these paradoxical results. In this paper, we show three paradoxical cases. (i) The successive "tossing" of a single fair quantum coin gives a biased result, a previously known result. (ii) The random tossing of two quantum coins, each with successive biased expectations, gives an average random walk position of approximately zero. (iii) The sequential periodic tossing of two quantum coins, each with successive negative biased expectations, gives an average random walk with positive expectation. Using these results, we then propose a protocol for identifying and classifying quantum operations that span the same Hilbert space for a two-level quantum system.

DOI: 10.1103/PhysRevE.101.052212

I. INTRODUCTION

Parrondo's games follow the structure Game A + Game B = Game C, for which A and B are losing games and C is a winning game, also known as Parrondo's paradox. Two biased games are designed such that the player loses capital in the long run if he chooses to play each game individually. However, if the player decides to play the games randomly or in a certain sequence, then, it is possible for the player to gain capital in the long run [1,2]. This paradoxical result has found its way to explaining a wider class of problems beyond game theory. In fact, these games now take a wider definition dependent on its field of applications to describe two dynamical systems combining to give a paradoxical result. For example, this paradoxical result can be found in nonlinear dynamics, whereby the combination of chaotic systems [3,4] in a certain manner gives rise to an ordered system.

Parrondo's paradox has also been applied to model ecological behavior, evolutionary biology, and population dynamics [5–11] as part of the survival strategies, in which individual strategy leads to the eventual decrease of population of the species. However, a periodic alternation of the two survival strategies leads to a long-term growth of the population. Parrondo's paradox has been used to explain the underlying dynamics of many other biological phenomena [12], the field of economics (game theory) [1,13,14], computer science [15], physical chemistry [16], and engineering optimization [17,18]. Besides its theoretical advancements [19–25], specific problems in social dynamics [26] and evolutionary biology [27] have been modeled and explained in terms of the paradox. More applications and the theoretical developments of the paradox can be found in the reviews in [12,28].

Many applications have also been linked to quantum models, where the classical coin toss is replaced by the measurement of a qubit. One of the studies is by Meyer and Blumer [29], in which they show that Parrondo's paradox can be modeled by probabilistic lattice gas automata. Their work introduces a quantum analog of the ratcheting mechanism seen in the original Parrondo's game, with possible applications in quantum computing. There have been further investigations of quantum Parrondo's games over the years, yielding other variants and in the process shedding light on the roles of entanglement and coherence in game outcomes. Quantum algorithms have been used to demonstrate the application of Parrondo's paradox in quantum game theory [29–39]. Of particular interest in quantum algorithms are quantum walks. The quantum random walk algorithm was previously developed with applications to quantum optics [40]. Since then, it has been at the forefront of development in quantum computation [41–43]. There have been attempts to computationally simulate quantum random walks via coin toss [44]; however, they do not fully identify or explain the paradoxical outcome arising from these computational simulations.

In this paper, we motivate the paradox by first introducing the mechanism behind random walks and quantum coin flips in the following sections. The general framework of a quantum coin toss will be discussed adequately for the understanding of the protocol used with the background information given in Refs. [44–46]. Then, we introduce three paradoxical results involving the quantum coin toss as a decision-making tool for random walks in Sec. II. The main contributions of our work are as follows:

*Corresponding author: kanghao_cheong@sutd.edu.sg

 ©2020 American Physical Society

(1) The successive "tossing" of a single fair quantum coin gives a biased result.

(2) The random tossing of two quantum coins, each with successive biased expectations, gives an average random walk position of approximately zero.

(3) The sequential periodic tossing of two quantum coins, each with successive *negative* biased expectations, gives an average random walk with positive expectation.

Lastly, we discuss the applicability of our result as a means of identifying the state of the initial qubit and the fairness of quantum coins.

A. Discrete classical walk

Consider a discrete walk along $x \in \mathbb{Z}$, purely determined by the result of a fair coin toss. A fair coin toss has two possible outcomes, *heads* (+1) and *tails* (−1), with a probability of each outcome being $\frac{1}{2}$. The probability distribution of a classical discrete walk determined by a fair coin toss can be visualized using a tableau. The symmetric entries of Table I imply that the mean position of the discrete classical walk is always zero, $\langle x\rangle_C = 0$. Here, the subscript C denotes the expected position in the *classical* regime. The same discrete classical walk can also be performed using a biased coin; however, the mean position will be biased towards the coin face that has a higher occurrence probability.

TABLE I. Probabilities for each position in a classical walk determined by a coin toss for $m \in [0, 4]$ steps.

	−4	−3	−2	−1	0	1	2	3	4
$m = 0$					1				
$m = 1$				$\frac{1}{2}$		$\frac{1}{2}$			
$m = 2$			$\frac{1}{4}$		$\frac{1}{2}$		$\frac{1}{4}$		
$m = 3$		$\frac{1}{8}$		$\frac{3}{8}$		$\frac{3}{8}$		$\frac{1}{8}$	
$m = 4$	$\frac{1}{16}$		$\frac{1}{4}$		$\frac{3}{8}$		$\frac{1}{4}$		$\frac{1}{16}$

B. Discrete quantum walk

Suppose we have a quantum process with basis state $|n, s\rangle$. The Hilbert space of this state is $\mathcal{H} = \mathcal{H}_x \otimes \mathcal{H}_c$, where $\mathcal{H}_x = \text{span}\{|n\rangle : n \in \mathbb{Z}\}$, n indicates the position along the x axis, and $\mathcal{H}_c = \text{span}\{|0\rangle, |1\rangle\}$ indicates tails and heads, respectively. A transformation analogous to a discrete walk involves two operations. At each step, we have the following:

(1) A coin-flip transformation $\mathcal{C}$,

$$\begin{aligned}\mathcal{C}|n,0\rangle &= a|n,0\rangle + b|n,1\rangle,\\ \mathcal{C}|n,1\rangle &= c|n,0\rangle + d|n,1\rangle,\end{aligned} \tag{1}$$

satisfies $|a|^2 + |b|^2 = |c|^2 + |d|^2 = 1$, where $a, b, c, d \in \mathbb{C}$. Such a $\mathcal{C}$ can be represented as a superposition of Pauli matrices,

$$\mathcal{C} = \sum_{\mu=0}^{3} a_\mu \sigma_\mu = \begin{bmatrix} a & b \\ c & d \end{bmatrix}, \tag{2}$$

where σ_μ are the Pauli matrices and σ_0 is the identity matrix. $\mathcal{C}$ is normalized and, in general, noncommutative; that is, $[\mathcal{C}_i, \mathcal{C}_j] \neq 0$ for $i \neq j$.

(2) A shift transformation $\mathcal{S}$ is a unitary operator in $\mathcal{H}$,

$$\begin{aligned}\mathcal{S}|n,0\rangle &= |n-1,0\rangle,\\ \mathcal{S}|n,1\rangle &= |n+1,1\rangle.\end{aligned} \tag{3}$$

One step of the random walk is given by $\mathcal{SC}$. Thus, in general, the entire transformation is unitary and combines the coin-flip transformation and shift transformation, given by

$$\mathcal{U} = \mathcal{S}\Big(\mathcal{C} \otimes \mathcal{I}_p\Big), \tag{4}$$

where $\mathcal{I}_p$ is the identity operator of size $p \times p$. The initial state of the system is $|\psi\rangle_0$, and N steps are taken by applying the unitary operator N times,

$$|\psi\rangle_N = \mathcal{U}^N |\psi\rangle_0. \tag{5}$$

For the purpose of discussion in this paper, we choose $|\psi\rangle_0 = |0, 0\rangle$ and two possible matrices $\mathcal{C}$, in the space $\mathcal{H}_x$, that satisfy the physical properties of a coin flip. This allows us to present a minimum working example that exhibits the paradoxical outcomes. The matrices are

$$\mathcal{C}_A = \frac{1}{\sqrt{2}}\begin{bmatrix} 1 & 1 \\ 1 & -1 \end{bmatrix}, \quad \mathcal{C}_B = \frac{1}{\sqrt{2}}\begin{bmatrix} -1 & -i \\ i & 1 \end{bmatrix}. \tag{6}$$

It is easy to check that both coin-flip transformations are fair when applied to an initial state. Consider the coin-flip transformation provided by the Hadamard operator $\mathcal{C}_A$ from Eq. (6).

$$\begin{aligned}
&\text{Step 1: } \mathcal{SC}_A|0,0\rangle = \frac{1}{\sqrt{2}}|-1,0\rangle + \frac{1}{\sqrt{2}}|1,1\rangle,\\
&\text{Step 2: } (\mathcal{SC}_A)^{\otimes 2}|0,0\rangle = \mathcal{SC}_A\Big[\frac{1}{\sqrt{2}}|-1,0\rangle + \frac{1}{\sqrt{2}}|1,1\rangle\Big] = \frac{1}{2}|-2,0\rangle + \frac{1}{2}|0,1\rangle + \frac{1}{2}|0,0\rangle - \frac{1}{2}|2,1\rangle,\\
&\text{Step 3: } (\mathcal{SC}_A)^{\otimes 3}|0,0\rangle = \frac{1}{2\sqrt{2}}|-3,0\rangle + \frac{1}{2\sqrt{2}}|-1,1\rangle + \frac{1}{\sqrt{2}}|-1,0\rangle - \frac{1}{2\sqrt{2}}|1,0\rangle + \frac{1}{2\sqrt{2}}|3,1\rangle,\\
&\text{Step 4: } (\mathcal{SC}_A)^{\otimes 4}|0,0\rangle = \frac{1}{4}|-4,0\rangle + \frac{3}{4}|-2,0\rangle + \frac{1}{4}|-2,1\rangle - \frac{1}{4}|0,0\rangle + \frac{1}{4}|0,1\rangle\rangle + \frac{1}{4}|2,0\rangle - \frac{1}{4}|2,1\rangle - \frac{1}{4}|4,1\rangle.
\end{aligned} \tag{7}$$

After four coin tosses [Eq. (7)], we obtain a distribution that differs from the classical coin toss. The possible positions and corresponding probabilities are $P(x=-4) = \frac{1}{16}$, $P(x=-2) = \frac{5}{8}$, $P(x=0) = \frac{1}{8}$, $P(x=2) = \frac{1}{8}$, and $P(x=4) = \frac{1}{16}$. The quantum coin toss has a net negative bias, and the mean position after four steps is $\langle x\rangle_Q = -0.111$. Here, the subscript

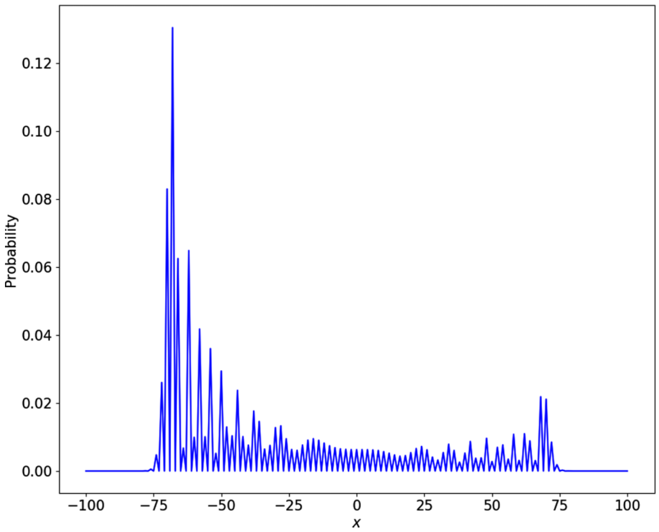

FIG. 1. Probability distribution of a quantum coin toss after $m = 100$ steps, with $\langle x\rangle_Q \approx -0.14416$.

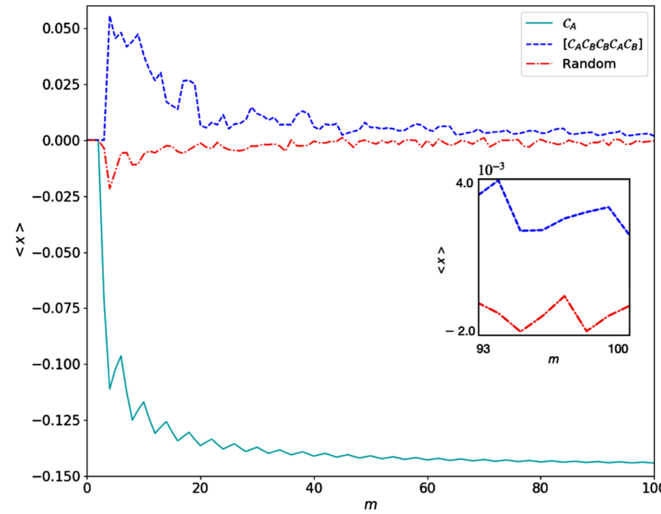

FIG. 2. Expected position when tossing two quantum coins $\mathcal{C}_A$ and $\mathcal{C}_B$ individually ($\langle x\rangle_Q \approx -0.14416$), randomly ($\langle x\rangle_Q \approx -0.00055$), and in a periodic sequence ($\langle x\rangle_Q \approx 0.00190$) for $m = 100$ steps, averaged over $N = 10^5$ games.

Q denotes the expected position in the *quantum* regime. The negative bias can be further shown by taking more steps. After $m = 100$ steps, the probability at each possible position can be computationally calculated. The probability distribution is plotted in Fig. 1, and the same result can be shown to exist for both matrices in Eq. (6). This is a known phenomenon, and more information can be found in Ref. [45]. This subject has attracted immense interest due to the unpredictable result when both $\mathcal{C}_A$ and $\mathcal{C}_B$ are used in a random and sequential periodic tossing.

II. PARADOXICAL QUANTUM WALK AND DISCUSSION

A. The paradoxes

In this section, we consider the paradoxical outcome of tossing two fair quantum coins given by $\mathcal{C}_A$ and $\mathcal{C}_B$ in Eq. (6). Figure 2 shows the expected position $\langle x\rangle_Q$ after $m = 100$ steps. The main results can be summarized as follows:

(1) The successive tossing of a single fair quantum coin gives a biased result.

(2) The random tossing of two quantum coins, each with successive biased expectations, gives an average random walk position of approximately zero.

(3) The sequential periodic tossing of two quantum coins, each with successive *negative* biased expectations, gives an average random walk with positive expectation. For sequential periodic tossing, we use the notation $[p_1, \dots, p_n]_r$, where the coin-tossing sequences is

$$\overbrace{\underbrace{\mathcal{C}_i \dots \mathcal{C}_i}_{p_1 \text{ times}} \dots \underbrace{\mathcal{C}_j \dots \mathcal{C}_j}_{p_n \text{ times}}}^{\text{length } r}$$

for $i, j \in \{A, B\}$, satisfying $\sum_{k=1}^{n} p_k = r$. For example, $[1, 2, 1, 1]_5$ represents a sequential periodic tossing of $\mathcal{C}_A\mathcal{C}_B\mathcal{C}_B\mathcal{C}_A\mathcal{C}_B$ or $\mathcal{C}_B\mathcal{C}_A\mathcal{C}_A\mathcal{C}_B\mathcal{C}_A$. In the case where both $\mathcal{C}$'s are fair, there is no need to distinguish between these two sequential periodic tossings for each representation.

All sequences of up to length 6 were numerically verified for positive expectation position after $m = 100$ steps. There are no sequences of length 6, satisfying the property; however, there exist two sequences of length 5 with positive expectation position after $m = 100$ steps. The sequences are $[1, 2, 1, 1]_5$ and $[1, 1, 2, 1]_5$.

B. Resolution to the three paradoxes

The resolution to the first paradox is a known result and included here for completeness. The paradox appears because of the underlying dynamics of quantum systems which can be attributed to the Copenhagen interpretation of a quantum state. In particular, (1) for *superposition*, a quantum qubit does not exist in distinct states but in all of its possible states at once, and (2) for *collapse of the wave function*, the wave function is a complete description of a quantum qubit. A measurement of the qubit causes the collapse of the wave function.

We give a few words of caution here. The superposition principle causes certain states to be amplified and others to destructively interfere, leading to these states being inaccessible. Consider the example in Sec. I B, in step 2 of Eq. (7): the wave function contains four possible states but only three possible outcomes $(-2, 0, 2)$. A measurement of these four states collapses this wave function into one of the three possible outcomes with the following probabilities: $P(x = -2) = \frac{1}{4}$, $P(x = 0) = \frac{1}{2}$, and $P(x = 2) = \frac{1}{4}$. Doing so destroys the quantum mechanical information associated with the coin bit. Now, in one of these distinct states, if we were to toss the same quantum coin for each of the states, we would obtain

$$\mathcal{SC}_A\big[\tfrac{1}{2}|-2, 0\rangle\big] \Rightarrow P(x = -3) = \tfrac{1}{8}, \quad P(x = -1) = \tfrac{1}{8};$$
$$\mathcal{SC}_A\big[\tfrac{1}{2}|0, 1\rangle\big] \Rightarrow P(x = -1) = \tfrac{1}{8}, \quad P(x = 1) = \tfrac{1}{8};$$
$$\mathcal{SC}_A\big[\tfrac{1}{2}|0, 0\rangle\big] \Rightarrow P(x = -1) = \tfrac{1}{8}, \quad P(x = 1) = \tfrac{1}{8};$$
$$\mathcal{SC}_A\big[-\tfrac{1}{2}|2, 1\rangle\big] \Rightarrow P(x = 1) = \tfrac{1}{8}, \quad P(x = 3) = \tfrac{1}{8}.$$

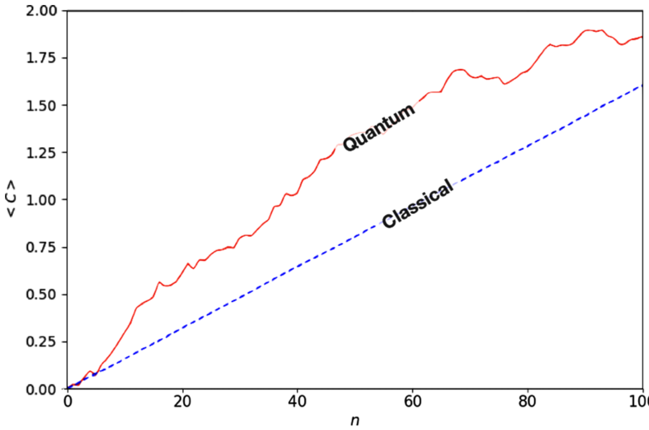

FIG. 3. The average capital $\langle C\rangle$ obtained by using the switching mechanism given by the quantum coin protocol with random switching ($m = 100$, $N = 10^3$) and a fair classical coin ($N = 10^6$), performed on a capital-dependent Parrondo's game described in [47]. N simulations were performed and averaged over for $n = 100$ such games. The quantum case exhibits fluctuations because it is averaged over a smaller number of simulations due to the increased complexity.

Once the state of $|n, s\rangle$ is measured after two tosses, a third toss gives the expected fair coin-toss result, where the probabilities of being in positions $n-1$ and $n+1$ are $\frac{1}{2}$. Adding up the probabilities of each possible position, we have $P(x=-3)=\frac{1}{8}$, $P(x=-1)=\frac{3}{8}$, $P(x=-1)=\frac{3}{8}$, and $P(x=3)=\frac{1}{8}$, which is identical to the classical result from Table I.

However, if the state is not measured after two tosses, it remains in a superposition of four possible states. A third toss leads to state $|-1,0\rangle$ being amplified, while state $|1,1\rangle$ destructively interferes, resulting in the state being inaccessible as in Eq. (7). This gives the quantum coin toss, after three steps, a negative bias. The quantum protocol is inherently fair, provided an observation is made after each step.

Furthermore, Fig. 2 predicts that the random tossing of two quantum coins, each with successive biased expectations, gives an average random walk position of approximately zero. The simulation results suggest that the random tossing of two quantum coins is analogous to the tossing of a single fair classical coin. This can be verified by using the probability density function of both the classical fair coin and the random tossing of two quantum coins for $m = 100$ as the decision-making tool to perform switching between two losing Parrondo's games. Figure 3 predicts positive expected capitals $\langle C\rangle$ in both cases for the capital-dependent Parrondo's game described in Ref. [1]. To obtain Fig. 3, we take the averaged capital of $N = 10^3$ simulations for the quantum coins and $N = 10^6$ for the classical coin. An increase in the average capital $\langle C\rangle$ over N simulations suggests a winning outcome. More importantly, the random tossing of two quantum coins can improve on the capital of the capital-dependent Parrondo's game.

The paradoxes can be resolved by considering the superposition principle in quantum states. The individual states and their amplitudes can be calculated at each step; such calculations will reveal the underlying dynamics that leads to the amplification and annihilation of individual states and a resolution of the paradoxical results.

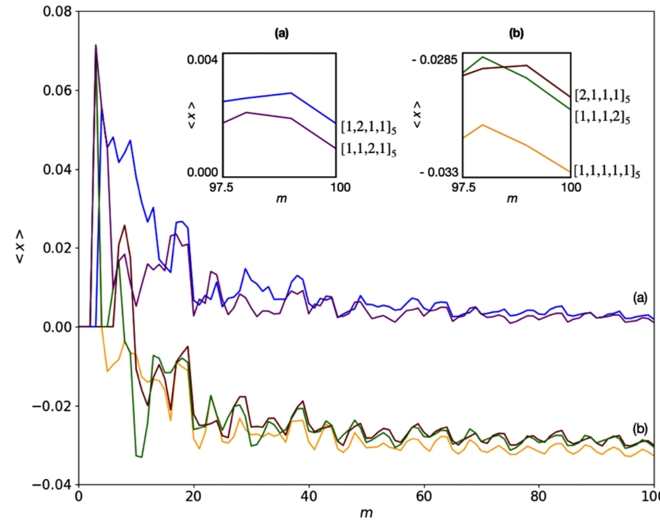

FIG. 4. The result obtained by sequential tossing of coins $[1, 2, 1, 1]_5$, $[2, 1, 1, 1]_5$, $[1, 1, 1, 1, 1]_5$, $[1, 1, 1, 2]_5$, and $[1, 1, 2, 1]_5$ for $m = 100$ steps. The expectation values are in Table II.

C. Discussion

There are further observations that can be made by following this quantum coin-toss protocol. Consider the transformations given by Eq. (6) and

$$\mathcal{C}_C = \frac{1}{\sqrt{3}}\begin{bmatrix} 1 & 1-i \\ 1+i & -1 \end{bmatrix}. \tag{8}$$

All three $\mathcal{C}$ have eigenvalues ± 1. Since the transformations have distinct eigenvalues and all three have similar eigenvalues, this implies that these matrices perform the same transformation, in our case, the coin-flip transformation. It is worth noting that while $\mathcal{C}_A$ and $\mathcal{C}_B$ are fair quantum coins, $\mathcal{C}_C$ is a biased coin.

Let us now examine the result of tossing two fair quantum coins. Consider a transient coin-toss sequence $\cdots\mathcal{C}_A\mathcal{C}_B\mathcal{C}_B\mathcal{C}_A\mathcal{C}_B\mathcal{C}_A\mathcal{C}_B\mathcal{C}_B\mathcal{C}_A\cdots$. One would expect that the sequences $[1, 2, 1, 1]_5$, $[2, 1, 1, 1]_5$, $[1, 1, 1, 1, 1]_5$, $[1, 1, 1, 2]_5$, and $[1, 1, 2, 1]_5$ for quantum coins C_A and C_B would give the same expected position as they represent the same transient choice of coin toss. However, since $[\mathcal{C}_A, \mathcal{C}_B] \neq 0$, the sequential periodic tossing gives different results (see Fig. 4 and Table II), differing from the dynamics of the classical case.

TABLE II. Expected position for sequential tossing of coins $[1, 2, 1, 1]_5$, $[2, 1, 1, 1]_5$, $[1, 1, 1, 1, 1]_5$, $[1, 1, 1, 2]_5$, and $[1, 1, 2, 1]_5$ for $m = 100$ steps.

Sequence	$\langle x\rangle_Q$	Sequence	$\langle x\rangle_Q$
$[1, 1, 1, 2]_5$	−0.03052	$[1, 2, 1, 1]_5$	0.001900
$[2, 1, 1, 1]_5$	−0.03008	$[1, 1, 2, 1]_5$	0.001028
$[1, 1, 1, 1, 1]_5$	−0.03273		

Additionally another important result comes from the invariance under switching of fair coins if they are tossed alongside another fair coin. In games where both quantum coins are fair, there is no need to distinguish which quantum coin is chosen first. That is, for the periodic tossing $[1, 2, 1, 1]_5$, both $\mathcal{C}_A\mathcal{C}_B\mathcal{C}_B\mathcal{C}_A\mathcal{C}_B$ and $\mathcal{C}_B\mathcal{C}_A\mathcal{C}_A\mathcal{C}_B\mathcal{C}_A$ give the same expected position after m tosses. The reason is because both fair quantum coins are representative of the same Hilbert space, but in different bases. The order in which the coins are tossed simply rewrites the basis of one coin into another for the same Hilbert space. The bases of the coin-flip transformations $\mathcal{C}_A$ and $\mathcal{C}_B$ are

$$\beta_A = \left\{ \begin{pmatrix} 1 \\ 1 \end{pmatrix}, \begin{pmatrix} 1 \\ -1 \end{pmatrix} \right\}, \quad \beta_B = \left\{ \begin{pmatrix} -1 \\ -i \end{pmatrix}, \begin{pmatrix} i \\ 1 \end{pmatrix} \right\},$$

respectively. Consider the coordinates represented by $\mathcal{C}_A$ and $\mathcal{C}_B$,

$$[\vec{a}_1]_A = \begin{pmatrix} \frac{1}{\sqrt{2}} \\ \frac{1}{\sqrt{2}} \end{pmatrix}, \qquad [\vec{a}_2]_A = \begin{pmatrix} \frac{1}{\sqrt{2}} \\ -\frac{1}{\sqrt{2}} \end{pmatrix}. \tag{9}$$

$$[\vec{a}_1]_B = \begin{pmatrix} -\frac{1}{\sqrt{2}} \\ -\frac{i}{\sqrt{2}} \end{pmatrix}, \qquad [\vec{a}_2]_B = \begin{pmatrix} \frac{i}{\sqrt{2}} \\ \frac{1}{\sqrt{2}} \end{pmatrix}, \tag{10}$$

satisfying

$$Q_j[\vec{a}_k]_i^{(j)} = [\vec{a}_k]_i, \tag{11}$$

where $[\vec{a}_k]_i^{(j)}$ are the coordinates in basis β_i represented in basis β_j. Q_j is the change in the basis matrix, $i, j \in \{A, B\}$, $k \in \{1, 2\}$. The change in basis matrix Q_j is a composition of basis β_j. The coordinates in the basis of one can be represented as a superposition of the basis of another:

$$\begin{aligned} [\vec{a}_1]_B^{(A)} &= \tfrac{1}{2}(-[\vec{a}_1]_A - i[\vec{a}_2]_A), \\ [\vec{a}_2]_B^{(A)} &= \tfrac{1}{2}(i[\vec{a}_1]_A + [\vec{a}_2]_A), \\ [\vec{a}_1]_A^{(B)} &= \tfrac{1}{2}([\vec{a}_1]_B + [\vec{a}_2]_B), \\ [\vec{a}_2]_A^{(B)} &= \tfrac{1}{2}([\vec{a}_1]_B - [\vec{a}_2]_B). \end{aligned}$$

The coefficients of the transformation are simply the scaled entries of Q_j (i.e., scaled by 0.5). This implies that the quantum superposition of states under the coin-flip transformation C_i is a linear combination of the coordinates of C_j. Thus, when the coin C_i is chosen, the information prior to the toss of that coin is preserved and simply represented in a different basis.

On the contrary, the same cannot be said for games played using a fair quantum coin and a biased quantum coin. In general, the periodic tossings have different $\langle x\rangle_Q$, and one coin cannot be switched for the other. For example, referring to Fig. 5, $\mathcal{C}_A\mathcal{C}_C\mathcal{C}_C\mathcal{C}_A\mathcal{C}_C$ and $\mathcal{C}_C\mathcal{C}_A\mathcal{C}_A\mathcal{C}_C\mathcal{C}_A$ have $\langle x\rangle_Q \approx -0.03864$ and $\langle x\rangle_Q \approx -0.03352$, respectively, after $m = 100$ steps. Thus, the sequence $[1, 2, 1, 1]_5$ must be distinguished. Furthermore, simply switching $\mathcal{C}_A$ with $\mathcal{C}_B$, both being fair coins, does not yield the same result when played alongside the biased coin $\mathcal{C}_C$, as can clearly be seen.

The method introduced here can be used as a protocol to computationally identify and classify quantum operations that span the same Hilbert space for a two-level quantum system. Furthermore, the choice of initial state is found to be important as well to produce the paradox. For example, if the start state were chosen to be $\frac{1}{\sqrt{2}}[i|0, 0\rangle + |0, 1\rangle]$, then $\langle x\rangle_Q = 0$ under quantum coin toss $\mathcal{C}_A$. This additionally enhances the use of this protocol in distinguishing the start states in quantum random walk coin-toss protocols.

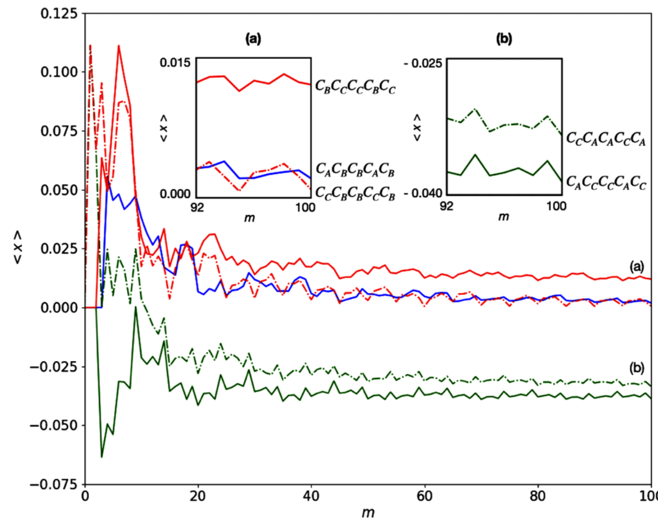

FIG. 5. Average position in a random walk after $m = 100$ steps for biased and unbiased coin sequences of the form $[1, 2, 1, 1]_5$, using pairwise combinations of $\mathcal{C}_A$, $\mathcal{C}_B$, and $\mathcal{C}_C$.

III. CONCLUSION

This paper introduced three paradoxical results derived from the quantum coin-toss random walk, played in the Parrondo's game format Game A + Game B = Game C. Of particular interest are the second and third paradoxes as they follow the general form of Parrondo's games.

These paradoxes give a glimpse of the unpredictable nature of quantum mechanics, which, when translated into quantum games, may display outcomes that differ from classical expectations. As the choice of the coin is not unique, the results presented can be generalized, except for choices of $\mathcal{C}$ that share the same eigenvectors discussed in this paper. While it does appear that the choice of $\mathcal{C}$ is arbitrary in Eq. (6), it is actually not so. Suppose there is a new matrix $\mathcal{C}_J$ that has the same eigenvectors as matrices $\mathcal{C}_A$ and $\mathcal{C}_B$; it can be used to replace either $\mathcal{C}_A$ or $\mathcal{C}_B$ to produce the same result. Otherwise, the results will wildly differ, for which there are an infinite number of possibilities to classify them all. This result can be used as a means of distinguishing operations in quantum computing, as well as to probe the initial qubit state.

As an outlook towards extending this work, the results presented in this paper may open up possibilities into the occurrence of Parrondo's paradox to quantum systems, with possible extensions to mixed or entangled states as the initial state, and provide insights into the classical limit of quantum game theory. As this is still a relatively new field of study, we foresee that theoretical extensions of such work could galvanize the work already done in quantum computing and information theory. Furthermore, this work has great relevance in explaining phenomena in quantum many-body systems and decoherence and could improve quantum computing protocols.

[1] G. P. Harmer and D. Abbott, Nature (London) **402**, 864 (1999).
[2] J. M. R. Parrondo, G. P. Harmer, and D. Abbott, Phys. Rev. Lett. **85**, 5226 (2000).
[3] L. Kocarev and Z. Tasev, Phys. Rev. E **65**, 046215 (2002).
[4] C.-H. Chang and T. Y. Tsong, Phys. Rev. E **67**, 025101(R) (2003).
[5] K. H. Cheong, J. M. Koh, and M. C. Jones, Proc. Natl. Acad. Sci. USA **115**, E5258 (2018).
[6] J. M. Koh, N.-g. Xie, and K. H. Cheong, Nonlinear Dyn. **94**, 1467 (2018).
[7] Z.-X. Tan and K. H. Cheong, Nonlinear Dyn. **98**, 1 (2019).
[8] K. H. Cheong, J. M. Koh, and M. C. Jones, Fluctuation Noise Lett. **18**, 1971001 (2019).
[9] Z. X. Tan and K. H. Cheong, eLife **6**, e21673 (2017).
[10] Z.-X. Tan, J. M. Koh, E. V. Koonin, and K. H. Cheong, Adv. Sci. **7**, 1901559 (2020).
[11] K. H. Cheong, Z. X. Tan, and Y. H. Ling, Commun. Nonlinear Sci. Numer. Simul. **60**, 107 (2018).
[12] K. H. Cheong, J. M. Koh, and M. C. Jones, BioEssays **41**, 1900027 (2019).
[13] J. M. Koh and K. H. Cheong, Nonlinear Dyn. **98**, 943 (2019).
[14] J. M. Koh and K. H. Cheong, Nonlinear Dyn. **96**, 257 (2019).
[15] G. P. Harmer, D. Abbott, P. G. Taylor, C. E. Pearce, and J. M. Parrondo, in *Stochastic and Chaotic Dynamics in the Lakes: Stochaos*, edited by P. V. E. McClintock, D. S. Broomhead, T. Mullin, and E. A. Luchinskaya, AIP Conf. Proc. No. 502 (AIP, New York, 2000), pp. 544–549.
[16] D. C. Osipovitch, C. Barratt, and P. M. Schwartz, New J. Chem. **33**, 2022 (2009).
[17] J. M. Koh and K. H. Cheong, J. Electron Spectrosc. Relat. Phenom. **227**, 31 (2018).
[18] K. H. Cheong and J. M. Koh, Ultramicroscopy **202**, 100 (2019).
[19] G. P. Harmer and D. Abbott, Fluctuation Noise Lett. **2**, R71 (2002).
[20] L. J. Gunn, A. Allison, and D. Abbott, Int. J. Mod. Phys.: Conf. Ser. **5111**, 344 (2003).
[21] W. W. M. Soo and K. H. Cheong, Phys. A (Amsterdam, Neth.) **412**, 180 (2014).
[22] W. W. M. Soo and K. H. Cheong, Phys. A (Amsterdam, Neth.) **392**, 17 (2013).
[23] K. H. Cheong and W. W. M. Soo, Phys. A (Amsterdam, Neth.) **392**, 4727 (2013).
[24] R. Zadourian, D. B. Saakian, and A. Klümper, Phys. Rev. E **94**, 060102(R) (2016).
[25] K. H. Cheong, D. B. Saakian, and R. Zadourian, Phys. Rev. E **96**, 062303 (2017).
[26] Y. Ye, K. H. Cheong, Y.-w. Cen, and N.-g. Xie, Sci. Rep. **6**, 37028 (2016).
[27] K. H. Cheong, Z. X. Tan, N.-g. Xie, and M. C. Jones, Sci. Rep. **6**, 34889 (2016).
[28] D. Abbott, Fluctuation Noise Lett. **9**, 129 (2010).
[29] D. A. Meyer and H. Blumer, J. Stat. Phys. **107**, 225 (2002).
[30] J. W. Lai and K. H. Cheong, Nonlinear Dyn. **100**, 849 (2020).
[31] A. Flitney and D. Abbott, Phys. A (Amsterdam, Neth.) **324**, 152 (2003).
[32] D. A. Meyer, Noisy quantum Parrondo games, in *Fluctuations and Noise in Photonics and Quantum Optics*, Vol. 5111, edited by D. Abbott, J. H. Shapiro, and Y. Yamamoto (SPIE, 2003), pp. 344–350.
[33] P. Gawron and J. A. Miszczak, Fluctuation Noise Lett. **5**, L471 (2005).
[34] J. Košík, J. Miszczak, and V. Bužek, J. Mod. Opt. **54**, 2275 (2007).
[35] A. P. Flitney, J. Ng, and D. Abbott, Phys. A (Amsterdam, Neth.) **314**, 35 (2002).
[36] S. Khan, M. Ramzan, and M. Khan, Int. J. Theor. Phys. **49**, 31 (2010).
[37] S. A. Bleiler and F. S. Khan, Phys. Lett. A **375**, 1930 (2011).
[38] D. Bulger, J. Freckleton, and J. Twamley, New J. Phys. **10**, 093014 (2008).
[39] Ł. Pawela and J. Sładkowski, Phys. D (Amsterdam, Neth.) **256**, 51 (2013).
[40] Y. Aharonov, L. Davidovich, and N. Zagury, Phys. Rev. A **48**, 1687 (1993).
[41] J. Kempe, Contemp. Phys. **44**, 307 (2003).
[42] A. Ambainis, Int. J. Quantum Inf. **1**, 507 (2003).
[43] M. Montero, Phys. Rev. A **95**, 062326 (2017).
[44] L. Yuwana, A. Purwanto, and E. Endarko, J. Inf. Math. Sci. **10**, 23 (2018).
[45] N. Shenvi, J. Kempe, and K. B. Whaley, Phys. Rev. A **67**, 052307 (2003).
[46] A. Nayak, J. Sikora, and L. Tunçel, Math. Program. **156**, 581 (2016).
[47] G. P. Harmer, D. Abbott, P. G. Taylor, and J. M. Parrondo, in *Unsolved Problems of Noise and Fluctuations: UPoN'99: Second International Conference*, edited by D. Abbott and L. B. Kish, AIP Conf. Proc. No. 511 (AIP, New York, 2000), pp. 189–200.